Bull. Mater. Sci. (2020) 43:195
https://doi.org/10.1007/s12034-020-02155-x

A sensitive voltammetric sensor based on silver nanoparticles/carbon nitride nanotubes@graphene quantum dots/a novel organic liquid: determination of triclosan in wastewater

ONUR AKYILDIRIM
Department of Chemical Engineering, Faculty of Engineering and Architecture, Kafkas University, 36000 Kars, Turkey
onurakyildirim@gmail.com

MS received 26 February 2020; accepted 26 May 2020; published online 12 August 2020

Abstract. A new sensor approach based on silver nanoparticles (AgNPs)/carbon nitride nanotubes (C_3N_4NTs) @graphene quantum dots (GQDs)/5-nitro-2-(3-hydroxy-4-methoxybenzylidenamino)-thiazole (ILs) was presented for triclosan (TCS) detection in wastewater samples. X-ray diffraction method, scanning electron microscope, electrochemical impedance spectroscopy, transmission electron microscope and cyclic voltammetry methods were used for all nanomaterials' characterizations. The linearity range and the detection limit (LOD) were found as 1.0×10^{-11} to 1.0×10^{-8} M and 2.0×10^{-12} M, respectively. The nanocomposite-modified electrode was used for wastewater sample analysis in the presence of different agents.

Keywords. Triclosan; Schiff base; carbon nitride nanotubes; nanoparticles; wastewater.

1. Introduction

Schiff bases are synthesized in two steps. Structurally, in the first stage, it was condensed by the primary amine of the carbonyl group to obtain carbonyl amine intermediate. In the second stage, at the end of the dehydration of this carbonyl amine intermediate, Schiff base is formed [1]. There are many studies that are considered as major corrosion inhibitors due to the presence of Schiff bases, electronegative atoms such as nitrogen (N), oxygen (O), sulphur (S), imine group (C=N) and aromatic ring in molecules [2]. Schiff bases have been especially studied in detail due to the wide range of applications in different fields, such as science and industry [3–5]. In recent years, studies have shown that Schiff bases have biological effects such as antioxidant [6], antimicrobial [7], antitumour [8,9], herbicidal [10] and antifungal [11]. Schiff base compounds have been investigated because of their selectivity, sensitivity and synthetic elasticity to metallic ions [12,13]. Some of the compounds having structural similarities to natural biological materials have been used as models in biological macroscopic systems, dioxygen carriers, catalysts, radiopharmaceuticals, etc. to prevent cancer and medical substrates [14,15].

5-Chloro-2-(2,4-dichloro-phenoxy)-phenol, known as triclosan (TCS), is a non-ionic substance and is an antifungal, antibacterial and antimicrobial agent. It is widely used as a recorder or antiseptic for personal-care products at concentrations of 0.1–0.3% (w/w) for more than 50 years, such as skin creams, liquid soaps, deodorants, toothpastes, shampoos, as with other consumer products, including medical devices, food-stuffs, plastic materials, detergents, clothing, etc. [16–18]. Nevertheless, TCS has been found to show resistance to biodegradation, acute toxicity, relatively high lipophilicity and environmental persistence. Intercalarily, exposing of this compound in large quantities may cause neurotoxic and immunotoxic reactions, and skin irritation in humans [19]. Therefore, the European Commission has decided not to approve this compound for the use in human hygiene biocidal products (2016/110/EU). Recently, the use of triclosan in some cosmetic products or personal care is also prohibited by FDA (the Food and Drug Administration). On the other hand, USEPA (the United States Environmental Protection Agency) has described photodegradation products (chlorophenols and chloroform) as possible human carcinogens and a high degree of contaminants [20,21]. Owing to its widespread use and toxicity effect, it has been very important in recent years to develop simple, fast, selective and sensitive analytical methods for detecting and quantifying TCS in commercial formulations and trace environmental samples [21,22]. Different analytical methods have been reported to detect TCS using liquid chromatography-mass spectrometry (LC-MS), gas chromatography-tandem mass spectrometry, liquid chromatography/electrospray ionization tandem mass spectrometry, voltammetrics and surface plasmon resonance [19,22–25]. Nevertheless, much material consumptions, expensive equipments and troublesome extraction steps are involved in these methods [22]. In order to reduce these problems,

the economical, sensitive analytical methods are urgently needed for instant analysis of TCS. Many sensor systems have deficiencies in terms of precision, stability, repeatability and reusability. To resolve these problem, in terms of important electronic properties, carbon nitride materials containing graphitic carbon nitride (g-C_3N_4) and highly stable nanomaterials like graphene oxide (GO)/graphene quantum dots (GQDs) are generally used [26–28]. Therefore, numerous articles have been reported on obtaining ultrafine g-C_3N_4 (utg-C_3N_4), C_3N_4 NTs and GQDs used in sensor applications [28–32]. Especially, graphitic carbon nitride (g-C_3N_4) has great attention for sensor/biosensor applications. It is the allotrope of carbon nitride materials and currently significant in materials science [27,31,33].

There is weak van der waals interaction between the C–N layers of graphitic carbon nitride. Because of van der waals interactions between C–N layers, it is chemically stable in solvents such as water and o-dichlorobenzene. Hence, the improved selectivity and sensitivity of electrochemical sensors for trace detection of chemicals or other biological samples was obtained [34]. In addition, it is generally used as catalyst owing to its low cost, thermal stability, high surface area (2500 $m^2\ g^{-1}$) and feasibility on surface engineering. Finally, it is formed by polymerization of melamine and also prepared by electrodeposition on Si(100) substrate [35,36]. Recently, graphene/graphene oxide has been considered as 'rising star' carbon material because of its unique properties, including superior mechanical strength, low density and high heat conductance. Graphene sheets, which are smaller than 100 nm, are called as GQDs. The quantum confinement and edge effects of GQDs lead to various electronic, optoelectronic properties, large surface area and high conductivity. In addition, GQDs, consisting of a single atomic layer of nanosized graphite, have the excellent performances, such as large diameter and better surface grafting using π–π conjugation and surface groups. GQDs, smaller than graphene sheets, causes effective surface area and high electrochemical effect [37–40]. Metallic nanoparticles, especially noble metal nanoparticles, usually exhibit high electrocatalytic activities towards the target compounds [41].

In this study, AgNPs/C_3N_4NTs@GQDs was first prepared by means of hydrothermal treatment. After that, C_3N_4NTs@GQDs was functionalized with 2-aminoethanethiol (AET) *via* the affinity of silver–sulphur for binding AgNPs. An important electrochemical sensor based on AgNPs/C_3N_4NTs@GQDs/ILs was improved and then applied to determine the selective and sensitive detection of TCS in the presence of different agents. The linearity range and LOD were obtained as 1.0×10^{-11} to 1.0×10^{-8} M and 2.0×10^{-12} M, respectively. Later, the prepared sensor was examined for repeatability and stability. In this report, we propose an electrochemical sensor including AgNPs/C_3N_4NTs@GQDs composite for triclosan quantification. To our knowledge, simple, selective and sensitive TCS electrochemical detection and AgNPs/C_3N_4NTs@GQDs composite is not yet available. On the other hand, the nanomaterial was also prepared under hydrothermal conditions in this study. According to the findings, the minimal waste formation in the preparation of C_3N_4NTs was obtained. Moreover, cheaper, eco-friendly and highly efficient nanomaterial was also found. In addition, high-performance liquid chromatography and mass spectrometry methods were developed for the determination of TCS in the literature. However, of these methods had various negative factors such as material consumption, complexity and high cost. In addition, the sensitive electrochemical sensor was developed due to catalytic properties of carbon nitride materials and GQDs [42,43]. The stable and fast electrochemical sensor was also prepared owing to the high electron transfer and the chemical modifiability. Moreover, our developed sensor not only meets the industrial requirements, but also has advantages in small sample consumption. Hence, low consumption of chemicals and composite makes sensor environmentally friendly. Finally, this study also generates tools with socio-economic benefit which contributes to better health and quality of life.

2. Experimental

2.1 *Materials*

All reagents and solvents required for the study were taken from Aldrich, Merck AG and Fluka.

TCS is a lipophilic compound (as described below) that is soluble in water, such as an anion in sufficient alkaline pH. Therefore, its stock standard solutions (1 mg ml^{-1}) were obtained in a mixture of distilled water/ethanol (1:1). To prepare diluted TCS, Britton–Robinson buffer solutions (BR, pH 9.0) were used.

2.2 *Instrumentation*

Electrochemical performance properties were measured with IviumStat (USA). X-ray diffraction measurement was done using the A Rikagu Miniflex X-ray diffractometer. To obtain scanning electron microscope visuals, the ZEISS EVO 50 analytical microscope model was used. The melting point of the synthesized compound was determined by the Stuart melting point SMP30 device. Infrared spectrum was created by means of ALPHA-P BRUKER FT-IR device. ^{13}C- and ^{1}H-NMR spectroscopic data were recorded using a Bruker Ultrashield Plus Biospin spectrometer at 400 MHz (TMS as standard and deuterated dimethyl sulphoxide as solvent).

2.3 *Synthesis of ILs*

2-Amino-5-nitrothiazole (10 mmol) in acetic acid solvent (20 ml) was reacted with 3-hydroxy-4-methoxybenzaldehyde (10 mmol). The product was then evaporated *in vacuo* at

50–55°C. The resulting product was recrystallized several times with ethanol to form pure 5-nitro-2-(3-hydroxy-4-methoxybenzylideneamino)-thiazole compound, as yellow crystals. Yield: 2.73 g (97%); mp: 200°C; IR (KBr, υ, cm^{-1}): 3430 (OH), 1621 (C=N), 1504 and 1361 (NO_2); ^{1}H-NMR (400 MHz, DMSO-d_6): δ 3.88 (s, 3H, OCH_3), 7.13 (d, 1H, ArH; J = 8.00 Hz), 7.25 (s, 1H, ArH), 7.41 (d, 1H, ArH; J = 8.40 Hz), 8.78 (s, 1H, N=CH), 9.56 (s, 1H, thiazole C_4), 9.78 (s, 1H, OH); ^{13}C-NMR (100 MHz, DMSO-d_6): δ 55.81 (OCH_3), 111.64, 113.61, 124.27, 129.88, 135.33, 147.03 (Ar-C), 147.33 (thiazole C_5), 153.35 (N=CH), 173.44 (thiazole C_4), 191.39 (thiazole C_2) (scheme 1).

2.4 *Preparation of AgNPs/C_3N_4NTs@GQDs*

The bulk g-C_3N_4 was obtained by thermal polycondensation of melamine benefiting from the previous report [33]. Briefly, 5 g of melamine powder was added to an alumina crucible. Then, it was heated to 600°C with an increase rate of 3°C min^{-1} and kept in a semi-closed environment for 2 h. After the product is cooled down to its temperature, the pale yellow polymeric g-C_3N_4 obtained in bulk was powdered and used in convenience. Henceforward, the synthesized bulk g-C_3N_4 (100 mg) powder was ultrasonicized in water (100 ml) for about 12 h and utg-C_3N_4 nanosheets were created. The obtained suspension was centrifuged at 5000 rpm and the residual unexfoliated g-C_3N_4 particles were removed. Ultimately, the suspension was dried and obtained as a powder. After preparing the utg-C_3N_4 suspension (1.0 mg ml^{-1}), the suspension was exposed to hydrothermal treatment at 150°C for 24 h at a heat rate of 1°C min^{-1}. The final product was obtained by drying at 60°C for 24 h and thermal treatment at 120°C for 24 h, respectively. The product was denoted as C_3N_4NTs. GQDs were prepared according to the reports by Yola and Atar [44]. To prepare AgNPs, AgNPs were synthesized first by mixing 20 ml of 0.25 mM $AgNO_3$ and 0.25 mM $Na_3C_6H_5O_7$. While stirring, 0.6 ml of 10 mM $NaBH_4$ was added all at once and kept on stirring for 30 s [45]. To the immobilization of AgNPs, the protocol was performed according to the previous report [41].

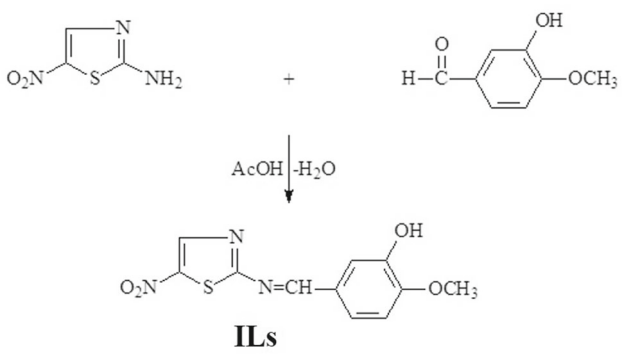

Scheme 1. Schematic diagram for synthesis of ILs.

To obtain C_3N_4NTs@GQDs nanocomposite, 35 mg C_3N_4NTs and 2 mg ml^{-1} of GQDs aqueous solution (5.0 ml) were sealed in a 20-ml Teflon autoclave for 60 min at 250°C. After the product cooled, the obtained nanocomposite of the C_3N_4NTs@GQDs was dried at room temperature. The immobilization of AgNPs on C_3N_4NTs@GQDs and the carboxylate groups were activated using 1-ethyl-3-(3-dimethyl aminopropyl) carbodiimide (EDC) [37]. C_3N_4NTs@GQDs were treated for 4 h with 0.2 M EDC solution. Then the interacted C_3N_4NTs@GQDs were treated with 1.0 mM AET (v:v, 1:1) for 2 h. AgNPs aqueous solution (1.0 mg ml^{-1}) was mixed with the functionalized C_3N_4NTs@GQDs (0.1 mg ml^{-1}) (v:v, 1:1) for 2 h. Consequently, the nanocomposite of AgNPs/C_3N_4NTs@GQDs was obtained.

2.5 *Electrode and sample preparation*

The carbon electrodes were cleaned according to the report [46]. The used electrode in this study such as AgNPs/C_3N_4NTs@GQDs/ILs-modified glassy carbon electrode (AgNPs/C_3N_4NTs@GQDs/ILs/GCE) was developed according to the report [46]. The sample was created according to the protocol in reference [22].

3. Results and discussion

3.1 *Nanostructures characterization*

The bulk structure was confirmed by SEM image of g-C_3N_4 (figure 1A). The bulk structure was seen with agglomeration, varying dimensions and irregular morphology of g-C_3N_4. After ultrasonication of g-C_3N_4, the utg-C_3N_4 nanolayers were prepared. The formation of utg-C_3N_4 nanolayers are observed from figure 1B. After hydrothermal treatment of utg-C_3N_4, the tubular structure of C_3N_4NTs appeared, as shown in figure 1C. Additionally, the diameters of open-ended C_3N_4NTs are within the range of 50–100 nm. The transmission electron microscope (TEM) image of the GQDs indicates the nano-sized and transparent structure without significant precipitation (figure 1D). After obtaining C_3N_4NTs-functionalized GQDs nanocomposite, the nano-linked and nanopore structure with cross-linking between GQDs and C_3N_4NTs is confirmed and shown in figure 1E. The presence of AgNPs on nanopore and nano-linked structure with cross-linking is verified, as shown in figure 1F. The average diameters of 5–10 nm are founded for AgNPs according to the structure analysis results. The EDX results are also given in figure 1G, and EDX analysis of the nanocomposite reveals Ag, C, N and O peaks. Hence, we can say that EDX analysis confirms the presence of these elements on AgNPs/C_3N_4NTs@GQDs nanocomposite.

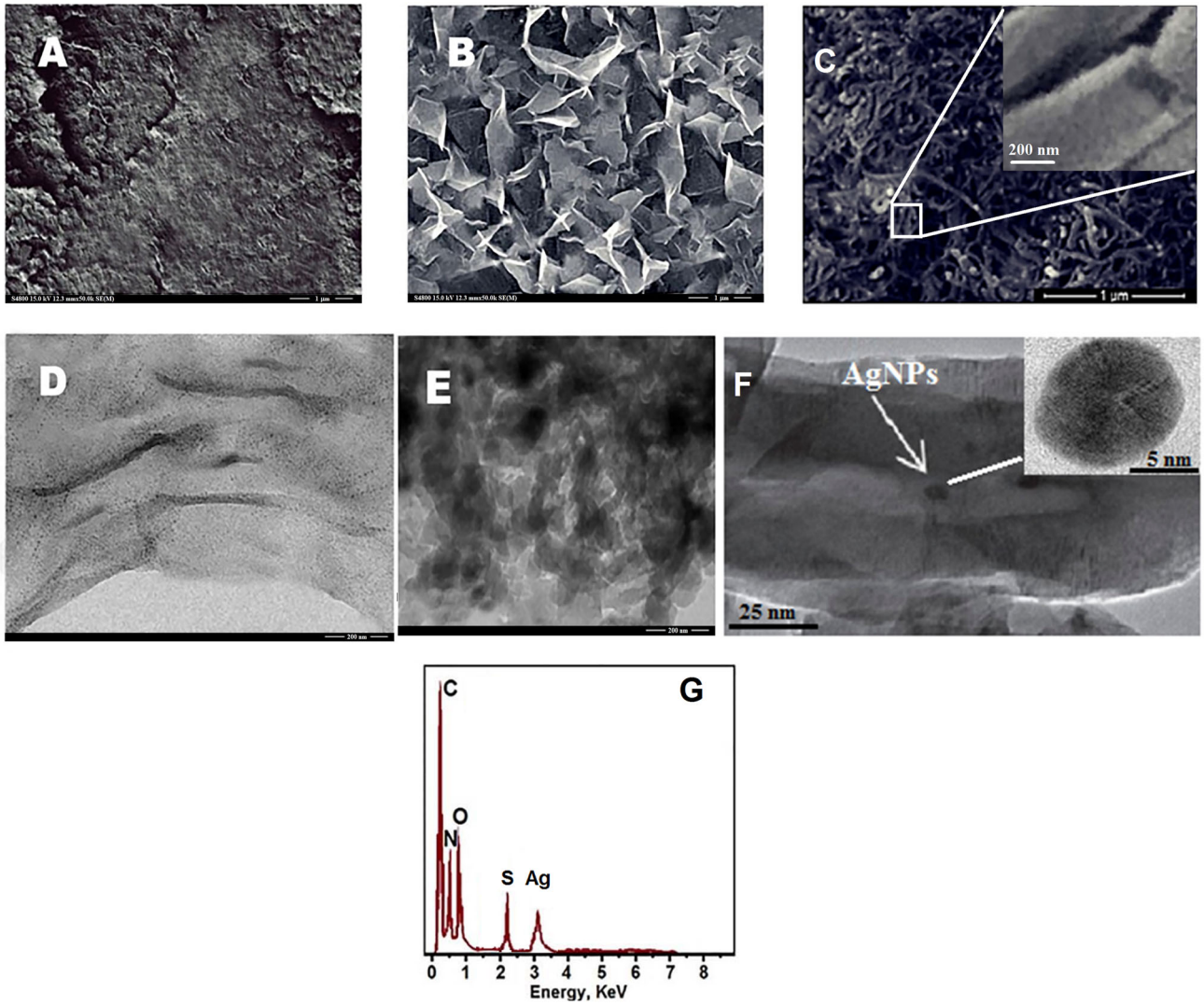

Figure 1. SEM images of (**A**) g-C_3N_4; (**B**) utg-C_3N_4 nanolayers; (**C**) C_3N_4NTs; (**D**) TEM images of GQDs; (**E**) C_3N_4NTs@GQDs; (**F**) AgNPs/C_3N_4NTs@GQDs (inset: TEM image of AgNPs) and (**G**) EDX analysis of the nanocomposite.

AgNPs/C_3N_4NTs@GQDs formation was confirmed by XPS analysis. The C–N and C–C coordinations of C_3N_4NTs are corresponded to the peaks at 285.1 and 284.3 eV, respectively (figure 2A) [32]. The nitrogen peaks demonstrate the binding energies at 401.3 and 398.8 eV, as shown in figure 2B [19,47]. The presence of AgNPs on the nanocomposite shows the characteristics binding energies of Ag $3d^{3/2}$ and $3d^{5/2}$. The binding energies at 374.5 and 373.2 eV are attributed to Ag $3d^{3/2}$ and $3d^{5/2}$, respectively. Therefore, the functionalization of silver with sulphur group of the AET on GQDs have been determined (figure 2C) [48]. The immobilization of AgNPs with thiol group is explained with XPS spectra according to the previous study [45]. In this paper, AgNPs/C_3N_4NTs@GQDs was first prepared by means of hydrothermal treatment. After that, C_3N_4NTs@GQDs was functionalized with AET *via* the affinity of silver–sulphur for binding AgNPs.

The characterized cyclic voltammetry (CV) and electrochemical impedance spectroscopy (EIS) structures of electrodes were performed and shown in figure 3. According to the CV results obtained (figure 3A), the peaks of 1.0 mM $[Fe(CN)_6]^{3-}$ with 160 mV of peak potential difference (ΔE_p) were determined at bare GCE (curve a). After modification of C_3N_4NTs@GQDs on bare GCE, ΔE_p decreased to 100 mV with an obvious increase in the peak signals (curve b). Owing to large surface area and thermal conductivity of C_3N_4NTs@GQDs, catalytic increases were observed according to the results obtained. Further catalytic increase was observed when using AgNPs/C_3N_4NTs@GQDs/ILs nanocomposite-modified GCE (ΔE_p = 60 mV) (curve c). This more catalytic effect on the application of the sensor was due to the fact that the AgNPs/C_3N_4NTs@GQDs/ILs nanocomposite facilitates the load transfer and the reduced mass transfer resistance on the

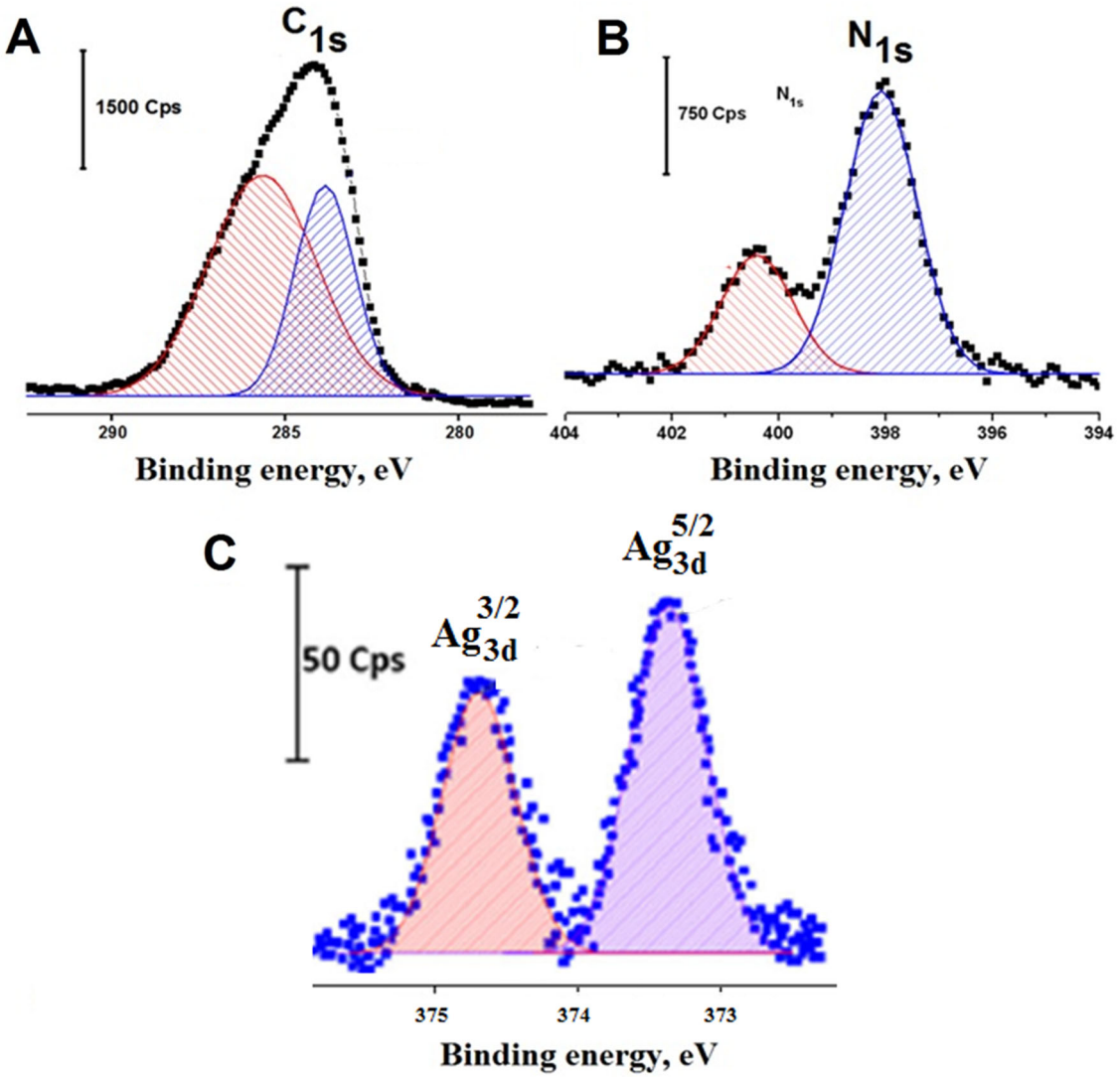

Figure 2. XPS spectra of AgNPs/C_3N_4NTs@GQDs.

electrode surface. The surface areas of bare GCE, C_3N_4NTs @GQDs/GCE and AgNPs/C_3N_4NTs@GQDs/ILs/GCE were obtained as 0.169, 0.692 and 1.402 cm^2, respectively. The results were confirmed by the data obtained by EIS experiments. EIS is an effective method for probing the features of surface-modified electrodes. It is capable of giving useful information about modified electrodes, the kinetics and mechanism of the film formation processes and surface coverage. Figure 3B shows the impedance plot (Nyquist diagram) of the bare GCE and different modified electrodes. The inset of figure 3B shows the experimental data obtained that are fitted to standard Randles equivalent circuits for AgNPs/C_3N_4NTs@GQDs/ILs/GCE surface analysis, which comprises the solution resistance (R_s), the charge transfer resistance (R_{ct}) and the constant phase element (CPE). The experimental impedance values are matched with Randles equivalent circuit simulation using Gamry software (EIS 600 Electrochemical Impedance Spectroscopy Software). According to the results observed in figure 3B, charge transfer resistance (R_{ct}) values are 55 (curve a), 90 (curve b) and 160 ohm (curve c), respectively. Therefore, CV results are highly consistent with R_{ct} values. According to CV and EIS experiments, the optimal electrochemical responses were obtained by using AgNPs/C_3N_4NTs@GQDs/ILs/GCE, which is caused by two obvious reasons: (1) the nanocomposite has some interesting properties such as multielectron transfer, thermal stability and low toxicity and (2) the nanocomposite has important π–π interaction and conjugation between analyte and GCE surface. Synergistic effect between GQDs and C_3N_4NTs increases the catalytic effect.

3.2 *pH effect*

The electrochemical oxidation mechanism of TCS at AgNPs/C_3N_4NTs@GQDs/ILs/GCE was investigated. The relationship between pH and anodic potential was observed

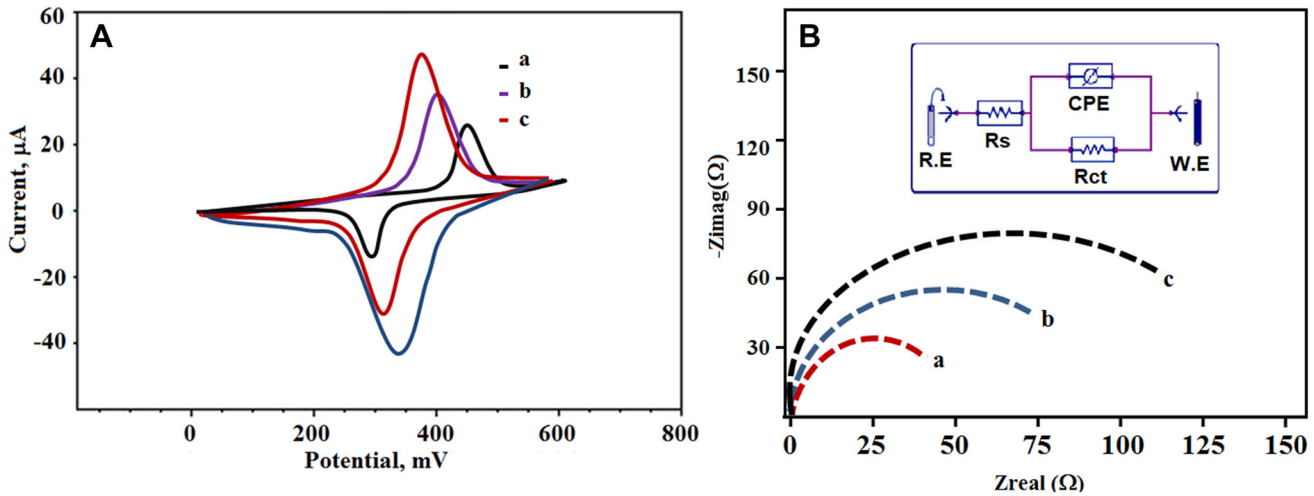

Figure 3. (**A**) Cyclic voltammograms at (a) bare GCE, (b) C_3N_4NTs@GQDs/GCE, (c) AgNPs/C_3N_4NTs@GQDs/ILs/GCE; (**B**) EIS response at (a) AgNPs/C_3N_4NTs@GQDs/ILs/GCE, (b) C_3N_4NTs@GQDs/GCE, (c) bare GCE; Redox probe: 1.0 mM $[Fe(CN)_6]^{3-}$ containing 0.1 M KCl, scan rate: 200 mV s^{-1}. RE stands for reference electrode and WE for working electrode.

to be $E_{pa} = 0.9422–0.04711$ pH for TCS. Because the number of electrons and protons in electrochemical oxidation is equal, it was observed that the slope value was close to the theoretical value of −0.062 mV per pH (figure 4). According to the differential pulse voltammetry (DPV) signals in the pH 4.0–10.0 range of TCS, the pH increased to 9.0 and it was observed that the signals remained constant or decreased after pH 9.0. Therefore, subsequent experiments were carried out at an optimum level at pH 9.0.

3.3 *Linearity range*

Figure 4 indicates the relation between current signals and TCS concentrations in AgNPs/C_3N_4NTs@GQDs/ILs/GCE (from 1.0×10^{-11} to 1.0×10^{-8} M). The regression equation is as follows: y (μA) = 9.4123x (nM) + 0.023 (according to figure 4). The detection limit (LOD) and the quantification limit (LOQ) for TCS were obtained as 1.0×10^{-11} and 2.0×10^{-12} M, respectively. The comparisons between the reported systems and the prepared sensor were made (table 1). The AgNPs/C_3N_4NTs@GQDs/ILs/GCE provides more precise analysis results with high selectivity. LOQ and LOD were estimated by equations (1 and 2):

$$\text{LOQ} = 10.0\,\text{S/m} \quad (1)$$

$$\text{LOD} = 3.3\,\text{S/m}, \quad (2)$$

where S is the standard deviation of the intercept and m the slope of the regression line (figure 5).

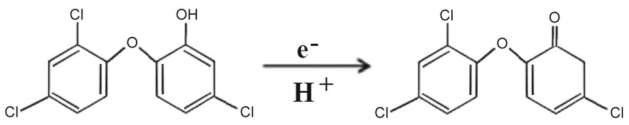

Figure 4. Electrochemical reaction of TCS at AgNPs/C_3N_4NTs @GQDs/ILs/GCE.

3.4 *Recovery*

According to the values shown in table 2, in consequence of close values to 100.00%, the developed sensor has high selectivity. In addition, standard addition method was

Table 1. Comparison of analytical performance values of AgNPs/C_3N_4NTs@GQDs/ILs/GCE for TCS determination with previously reported modified electrodes.

Materials	Linear range (M)	LOD (M)	Ref.
β-CNT/GNPs/GC	2.0×10^{-6} to 1.0×10^{-4}	6.0×10^{-7}	[49]
nZnO-MWCNT/GC	5.18×10^{-9} to 6.91×10^{-6}	4.49×10^{-9}	[50]
MWCNT/GC	1.03×10^{-5} to 1.49×10^{-4}	5.8×10^{-6}	[51]
AuNPs/POM/rGO/GC	5.0×10^{-10} to 5.0×10^{-8}	1.5×10^{-10}	[22]
MCM/SPS	2.76×10^{-9} to 1.38×10^{-7}	8.29×10^{-10}	[52]
CNP-PDDAC/ITO	5.0×10^{-7} to 5.0×10^{-5}	—	[53]
AgNPs/C_3N_4NTs@GQDs/ILs/GCE	1.0×10^{-12} to 1.0×10^{-8}	2.0×10^{-12}	This study

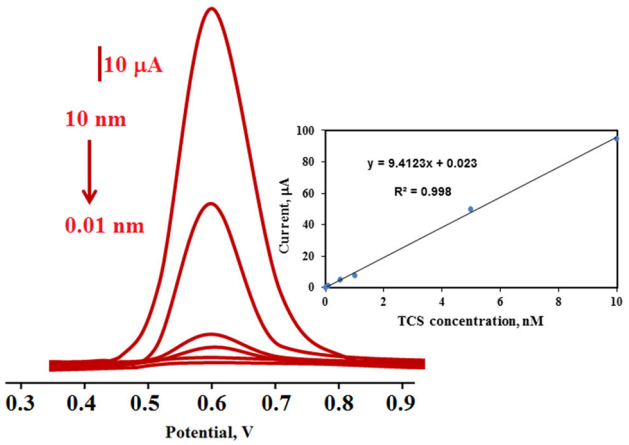

Figure 5. DPVs with different TCS concentrations in AgNPs/C_3N_4NTs@GQDs/ILs/GCE at pH 9.0 (from 1.0×10^{-11} to 1.0×10^{-8} M TCS). Inset: calibration curve of TCS.

Table 2. The recycling values of EZE (n = 7).

Sample	Added TCS (nM)	Found TCS (nM)	Recovery (%)
Wastewater samples	—	2.08 (±0.01)	—
	0.1	2.19 (±0.04)	100.46 ± 1.0
	0.5	2.60 (±0.07)	100.78 ± 0.7
	1.0	3.06 (±0.02)	99.35 ± 1.9

applied to the pharmaceutical preparations. The calibration equation is y (µA) = 9.4107x (nM) + 6.741 for AgNPs/C_3N_4NTs@GQDs/ILs/GCE. As a result, the matrix presence in pharmaceutical preparations have been found to not affect TCS selective analysis values too much.

3.5 *Selectivity, stability and repeatability of AgNPs/C_3N_4NTs@GQDs/ILs/GCE*

For the stability of AgNPs/C_3N_4NTs@GQDs/ILs/GCE, the signals of 10.0 nM TCS on AgNPs/C_3N_4NTs@GQDs/ILs/GCE were measured for 60 days and repeated signals were obtained at about 100.0 µA. Therefore, it has high stability in the pharmaceutical preparation analysis of the developed nanosensor. For repeatability test of AgNPs/C_3N_4NTs@GQDs/ILs/GCE in the presence of 10.0 nM TCS, 50 differential pulse voltammograms were received and the repeated signals were determined. The standard solution containing 10.0 nM TCS, 10.0 nM 2,4,6-trichlorophenol (TCP) and 10.0 nM p-chlorophenol (PCP) were prepared to show the selectivity of AgNPs/C_3N_4NTs@GQDs/ILs/GCE. According to figure 6, the current signals were shown at +0.61 V for TCS, 0.45 V for TCP and 0.52 V for PCP. The oxidation potentials are different and any interference effect is not obtained. According to figure 6 and recovery

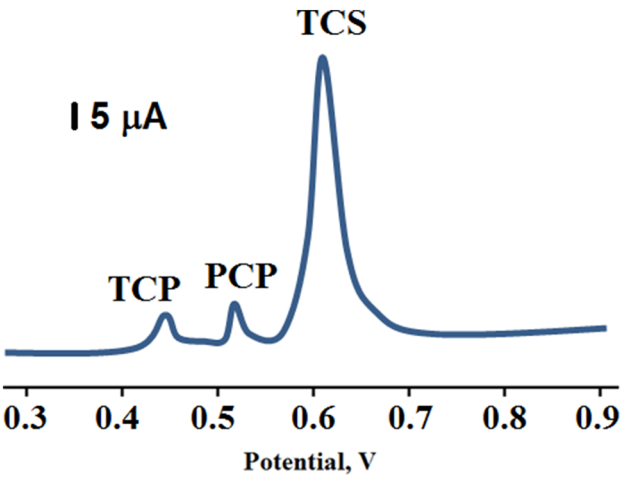

Figure 6. Square wave voltammograms at AgNPs/C_3N_4NTs@GQDs/ILs/GCE towards 10.0 nM TCS, 10.0 nM TCP and 10.0 nM PCP.

experiments, the selectivity of AgNPs/C_3N_4NTs@GQDs/ILs/GCE is very good for TCS detection.

4. Conclusions

In this report, novel, selective and sensitive electrochemical sensor depend on AgNPs/C_3N_4NTs@GQDs/ILs/GCE was developed and applied to determine the amount of triclosan in wastewater samples. The nanomaterials and surfaces created are well characterized using TEM, SEM, CV, EIS and EDX. In accordance with the characterization analysis, binding of AgNPs into C_3N_4NTs@GQDs is homogeneously distributed. This situation led to the formation of nanocomposite. The linearity range and the detection limit were calculated as 1.0×10^{-14} to 1.0×10^{-11} mM and 2.0×10^{-15}. The developed sensor was precise, stable and reusable. Because of all these results, we can say that the electrochemical sensor is used for triclosan determination.

Acknowledgement

We wish to thank all who assisted in conducting this study.

References

[1] da Silva C M, da Silva D L, Modolo L V, Alves R B, de Resende M A, Martins C V *et al* 2011 *J. Adv. Res.* **2** 1
[2] Patel A S, Panchal V A, Mudaliar G V and Shah N K 2013 *J. Saudi Chem. Soc.* **17** 53
[3] Gupta K and Sutar A K 2008 *Coord. Chem. Rev.* **252** 1420
[4] Prakash A and Adhikari D 2011 *Int. J. ChemTech. Res.* **3** 1891

[5] Brodowska K and Łodyga-Chruścińska E 2014 *Chemik* **68** 129
[6] Dileepan A B, Prakash T D, Kumar A G, Rajam P S, Dhayabaran V V and Rajaram R 2018 *J. Photochem. Photobiol. B* **183** 191
[7] Aktas-Yokus O, Yuksek H, Gursoy-Kol O and Alpay-Karaoglu S 2015 *Med. Chem. Res.* **24** 2813
[8] Alturiqi A S, Alaghaz A-N M and Ammar R A 2017 *J. Chin. Chem. Soc.* **64** 1270
[9] Asadi Z, Golchin M, Eigner V, Dusek M and Amirghofran Z 2018 *J. Photochem. Photobiol. Chem.* **361** 93
[10] Zhu S, Xu S, Yi X, Wang J, Zhao Z and Jiang J 2018 *Ind. Crops Prod.* **115** 111
[11] Patil R H, Kalam Khan F A, Jadhav K, Damale M, Akber Ansari S, Alkahtani H M *et al* 2018 *Arch. Pharm. (Weinheim)* **351** 1
[12] Gao W and Zheng Z 2002 *Molecules* **7** 511
[13] Shakir M, Azam M, Azim Y, Parveen S and Khan A U 2007 *Polyhedron* **26** 5513
[14] Andiappan K, Sanmugam A, Deivanayagam E, Karuppasamy K, Kim H-S and Vikraman D 2018 *Sci. Rep.* **8** 3054
[15] Utthra P P and Raman N 2018 *Int. J. Biol. Macromol.* **116** 194
[16] Snyder S A, Westerhoff P, Yoon Y and Sedlak D L 2003 *Environ. Eng. Sci.* **20** 449
[17] Peck A M 2006 *Anal. Bioanal. Chem.* **386** 907
[18] Montaseri H and Forbes P B 2016 *TrAC Trends Anal. Chem.* **85** 221
[19] Atar N, Eren T, Demirdögen B, Yola M L and Çağlayan M O 2015 *Ionics* **21** 2285
[20] Jones R D, Jampani H B, Newman J L and Lee A S 2000 *Am. J. Infect. Control* **28** 184
[21] Giuliano C A and Rybak M J 2015 *Pharmacother. J. Hum. Pharmacol. Drug Ther.* **35** 328
[22] Yola M L, Atar N, Eren T, Karimi-Maleh H and Wang S 2015 *RSC Adv.* **5** 65953
[23] Chu S and Metcalfe C D 2007 *J. Chromatogr. A* **1164** 212
[24] Wu J-L, Lam N P, Martens D, Kettrup A and Cai Z 2007 *Talanta* **72** 1650
[25] Vidal L, Chisvert A, Canals A, Psillakis E, Lapkin A, Acosta F *et al* 2008 *Anal. Chim. Acta* **616** 28
[26] Yola M L, Eren T and Atar N 2016 *J. Electrochem. Soc.* **163** B588
[27] Yola M L, Göde C and Atar N 2017 *Electrochim. Acta* **246** 135
[28] Mert S, Bankoğlu B, Özkan A, Atar N and Yola M L 2018 *J. Mol. Liq.* **254** 8
[29] Elçin S, Yola M L, Eren T, Girgin B and Atar N 2016 *Electroanalysis* **28** 611
[30] Akyıldırım O, Kardaş F, Beytur M, Yüksek H, Atar N and Yola M L 2017 *J. Mol. Liq.* **243** 677
[31] Yola M L and Atar N 2017 *Ind. Eng. Chem. Res.* **56** 7631
[32] Yola M L and Atar N 2017 *J. Electrochem. Soc.* **164** B223
[33] Yola M L and Atar N 2019 *Compos. Part B Eng.* **175** 107113
[34] Kıran T R, Atar N and Yola M L 2019 *J. Electrochem. Soc.* **166** H495
[35] Cao S, Low J, Yu J and Jaroniec M 2015 *Adv. Mater.* **27** 2150
[36] Gong Y, Li M, Li H and Wang Y 2015 *Green Chem.* **17** 715
[37] Yola M L and Atar N 2016 *J. Electrochem. Soc.* **163** B718
[38] Yola M L and Atar N 2018 *J. Electrochem. Soc.* **165** H1
[39] Shen J, Zhu Y, Yang X and Li C 2012 *Chem. Commun.* **48** 3686
[40] Mazloum-Ardakani M, Aghaei R, Abdollahi-Alibeik M and Moaddeli A 2015 *J. Electroanal. Chem.* **738** 113
[41] Beytur M, Kardaş F, Akyıldırım O, Özkan A, Bankoğlu B, Yüksek H *et al* 2018 *J. Mol. Liq.* **251** 212
[42] Taheri H, Unal M A, Sevim M, Gurcan C, Ekim O, Ceylan A *et al* 2020 *Small* **16** 1904619
[43] Yola M L and Atar N 2019 *Biosens. Bioelectron.* **126** 418
[44] Yola M L and Atar N 2018 *Appl. Surf. Sci.* **458** 648
[45] Yola M L, Eren T, Atar N, Saral H and Ermiş İ 2016 *Electroanalysis* **28** 570
[46] Atar N, Yola M L and Eren T 2016 *Appl. Surf. Sci.* **362** 315
[47] Atar N, Eren T, Yola M L, Karimi-Maleh H and Demirdögen B 2015 *RSC Adv.* **5** 26402
[48] Yola M L, Eren T, Atar N and Wang S 2014 *Chem. Eng. J.* **242** 333
[49] Li B, Qiu Z, Wan Q, Liu Y and Yang N 2014 *Phys. Status Solidi A* **211** 2773
[50] Moyo M, Florence L R and Okonkwo J O 2015 *Sens. Actuators B Chem.* **209** 898
[51] Baranowska I and Bijak K 2013 *J. Anal. Chem.* **68** 891
[52] Regiart M, Magallanes J L, Barrera D, Villarroel-Rocha J, Sapag K, Raba J *et al* 2016 *Sens. Actuators B Chem.* **232** 765
[53] Amiri M, Shahrokhian S, Psillakis E and Marken F 2007 *Anal. Chim. Acta* **593** 117